

THE HIGGS DISCOVERY POTENTIAL OF ATLAS

CHRISTOPHER COLLINS-TOOTH
for the ATLAS collaboration

*Department of Physics and Astronomy, University of Glasgow, Glasgow G12 8QQ,
Scotland*

Received 23 October 2007; Accepted 20 February 2008
Online 20 June 2008

Higgs boson production and decay at the LHC is described, together with related ATLAS search channels, in order to provide an overview of the ATLAS Higgs discovery potential.

PACS numbers: 14.80.Bn, 14.80.Cp

UDC 539.1.076

Keywords: Large Hadron Collider, Higgs boson, ATLAS

1. Introduction

The ATLAS detector [1] is one of two general purpose detectors under construction at the Large Hadron Collider (LHC), CERN, Switzerland. The LHC will begin to provide ATLAS with colliding beams, each of 7 TeV protons, in the summer of 2008. It is expected that a low-luminosity running phase will commence in 2009, with instantaneous luminosity (L) of $(1-2) \times 10^{33} \text{ cm}^{-2}\text{s}^{-1}$. The aim of this phase will be to gather approximately 30 fb^{-1} of integrated luminosity ($\int L dt$) by 2011. After this, L will be increased to approximately $10^{34} \text{ cm}^{-2}\text{s}^{-1}$, with the aim of gathering $\int L dt \sim 300 \text{ fb}^{-1}$ by 2014/2015. The ATLAS trigger will reduce the frequency of events saved for offline analysis to approximately 200 Hz.

Some important design features of ATLAS are its high hermeticity (vital in measurements of missing transverse energy), powerful tracking in the Inner Detector (useful for example, in b-tagging measurements), excellent Electromagnetic Calorimeter energy and angular resolution (e.g. for measurement of γ , e^\pm energies, and separation of γ/jet and γ/π^0). ATLAS is also designed to have excellent muon detection efficiency and momentum measurement, using the Inner Detector and the Muon Spectrometer. The nominal energy scales are $e/\gamma \sim 0.1\%$, $\mu \sim 0.1\%$, $\text{jets} \sim 1\%$.

2. Standard Model Higgs production and decay at the LHC

Figure 1 shows that by far the most important production mechanism over the entire mass search region for a Standard Model (SM) Higgs boson is gluon-gluon fusion. This production mechanism is followed in importance by vector boson fusion (VBF) at the 10 – 20% level, and Z/W-associated and associated-top production at a still lower cross-section.

The branching ratios for SM Higgs decay are also shown in Fig. 1. In the Higgs mass region $M_h < 125$ GeV, the primary decay mechanism is $h \rightarrow b\bar{b}$. At higher masses, decays to (initially off-shell) gauge bosons become dominant. This occurs first for W -bosons, and this decay stays dominant over the decay to Z -bosons, though the latter is preferred at higher masses ($M_h > 2M_Z$), because it has a very clean experimental signature.

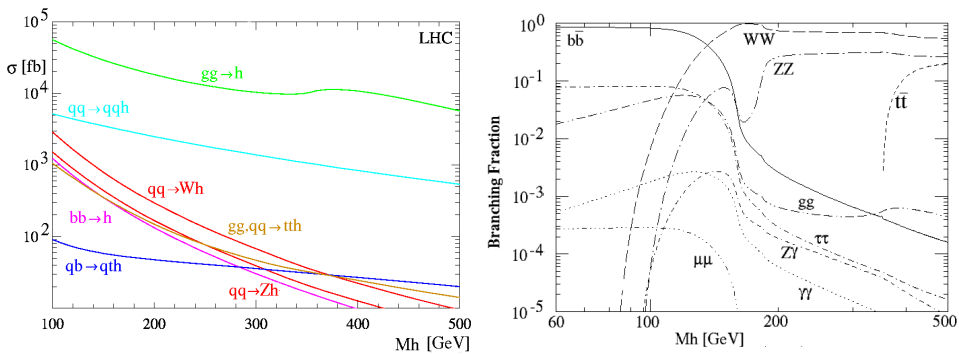


Fig. 1. SM Higgs production (left) [2] and decay (right) [3] at the LHC.

3. ATLAS Higgs sensitivity and searches

3.1. ATLAS SM Higgs sensitivity

ATLAS is optimised to cover a large spectrum of possible Higgs particles and their signatures. The ATLAS SM Higgs significances for the individual channels as a function of M_h are shown in Fig. 2 and also shown is the overall significance when multiple channels are considered. ATLAS should make a light Higgs discovery ($M_h < 180$ GeV) with $\int L dt = 30 \text{ fb}^{-1}$. Discovery in the region $M_h < 120$ GeV is clearly the most challenging for ATLAS, and will probably require several channels to be combined. Given a favourable Higgs mass, ATLAS could make a discovery with much less luminosity. By combining VBF, $h \rightarrow \gamma\gamma$, $t\bar{t}h \rightarrow b\bar{b}$ and ZZ^* , discovery of a Higgs with $M_h > 120$ GeV could be made with just 10 fb^{-1} of luminosity [4]. Above $M_h > 2M_Z$, two on-shell Z -bosons can be created, opening up the ‘gold plated’ channel $h \rightarrow ZZ \rightarrow 4l^\pm$.

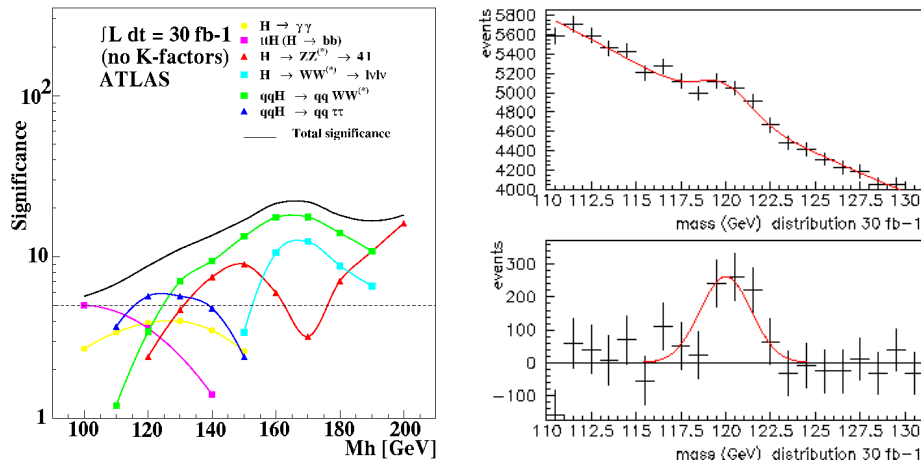


Fig. 2 (left). ATLAS sensitivity to the discovery of a SM Higgs boson for $\int L dt = 30 \text{ fb}^{-1}$ [4]. No K-factors have been applied.

Fig. 3. Reconstructed M_h for an input $M_h = 120 \text{ GeV}$ in the channel $h \rightarrow \gamma\gamma$ before (top) and after (bottom) background subtraction ($\int L dt = 30 \text{ fb}^{-1}$) [5].

3.2. $h \rightarrow \gamma\gamma$

This channel features a narrow mass peak over a smooth background, but as can be seen from Fig. 2, it is only useful at low M_h ($< 140 \text{ GeV}$). This is a benchmark channel for ATLAS detector performance, relying upon Electromagnetic Calorimeter resolution, but also accurate primary vertex determination. The irreducible background to this channel is the $\gamma\gamma$ continuum. Powerful rejection is needed to reduce jet-jet and γ -jet backgrounds, where the jet could be misidentified as a photon. When the analysis is performed using NLO production cross-sections [5], the ATLAS significance varies from 5.4 ($M_h = 140 \text{ GeV}$), through to 6.2 ($M_h = 130 \text{ GeV}$) and 6.1 ($M_h = 120 \text{ GeV}$) for 30 fb^{-1} of integrated luminosity. Figure 3 shows a mass distribution for an assumed $M_h = 120 \text{ GeV}$. The analysis makes use of photon conversion recovery, where for the approximately 40% of signal events when at least one photon converts, an 80% recovery rate is assumed.

3.3. $h \rightarrow ZZ^* \rightarrow 4l^\pm$

This channel has a clean signature, but low statistics ($30 - 110 \text{ fb}$ for $M_h = 130 - 200 \text{ GeV}$) [6]. It is another benchmark channel for detector performance, with the appearance of four high-transverse momentum (P_T) charged leptons testing the ATLAS momentum and energy resolution (via the Inner Detector, Muon Spectrometer and Electromagnetic Calorimeter). Mass peaks can be produced in this channel e.g. for $4e$, 4μ , $2e2\mu$ final states, which differ by resolution, but are typically in the range $1.5 - 2 \text{ GeV}$. The channel also provides a possibility of determining the spin and CP-eigenvalue of a SM Higgs [7]. The main backgrounds to the

channel are the irreducible $ZZ^* \rightarrow 4l^\pm$ continuum, and the (reducible) $t\bar{t} \rightarrow 4l + X$ and $Zb\bar{b} \rightarrow 4l + X$. These backgrounds contain non-isolated leptons with high impact parameters. Once selection is performed, the ZZ -continuum background is dominant. The shape and normalisation of these backgrounds will be obtained experimentally from data in order to minimise PDF and luminosity uncertainties. The ATLAS signal significance with no K -factors applied (for $\int Ldt = 30 \text{ fb}^{-1}$) rises above 5σ at $M_h \approx 130 \text{ GeV}$, and increases to approximately 9σ at $M_h \approx 150 \text{ GeV}$. The significance then drops below 5σ at $M_h \approx 160 \text{ GeV}$ [6].

3.4. Vector boson fusion $h \rightarrow WW^{(*)}$

In addition to being the second most important SM Higgs production mechanism after gluon-gluon fusion, VBF has a number of topological features which enable ATLAS to efficiently reject background. Due to this, the VBF channel $h \rightarrow WW^{(*)}$ in particular demonstrates large discovery potential over the region $125 < M_h < 190 \text{ GeV}$. VBF produces Higgs decay products which lie between two forward jets. These jets, with Higgs decay products located between them in pseudorapidity (η), coupled with an absence of jets in the central region (due to the absence of quark-quark colour exchange) provide the experimental signature of VBF. The two forward ‘tag jets’ typically have higher invariant dijet mass (M_{jj}) than the tag jets identified in QCD background processes, and so a cut on M_{jj} is also applied by ATLAS to improve background rejection.

In the $h \rightarrow WW^* \rightarrow l\nu l\nu$ channel, the leptons are spin-correlated to the Higgs resonance. For a SM Higgs boson, the charged leptons will emerge in the same direction as each other. This is yet another topological feature which improves background rejection. Due to the production of two neutrinos, only the transverse mass, $M_T = \sqrt{((E_T^{ll} + E_T^{\nu\nu})^2 - (p_T^{ll} + p_T^{miss})^2)}$ can be reconstructed. This distribution for signal having $M_h = 160$ in the $e\mu$ final state is shown in Fig. 4, along with the relevant background distributions.

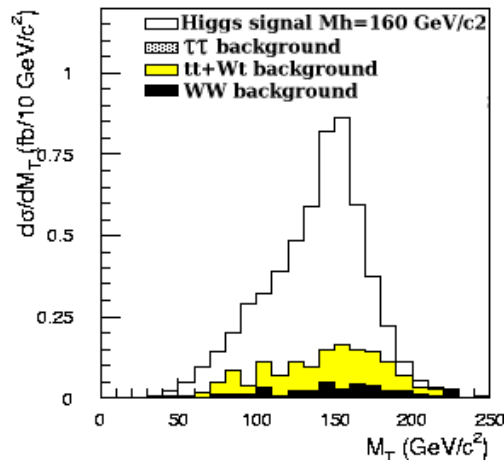


Fig. 4. Distribution of the transverse mass M_T for a SM Higgs boson mass of 160 GeV in the $h \rightarrow WW^* \rightarrow l\nu l\nu$ ($e\mu$) channel after all selection cuts are applied [4].

With $\int Ldt = 10 \text{ fb}^{-1}$, the ATLAS signal significance at $M_h = 160 \text{ GeV}$ for the $\nu\nu\nu$ final state reaches approximately 8.1σ for the $e\mu$ channel, and approximately 7.4σ in the $ee/\mu\mu$ channel. The νjj final state is also considered by ATLAS, and provides a significance of 4.6 at $M_h = 160 \text{ GeV}$ for $\int Ldt = 30 \text{ fb}^{-1}$. With $\int Ldt = 10 \text{ fb}^{-1}$, the ATLAS signal significance for the combination of considered $\nu\nu\nu$ and νjj channels is above 5σ for $135 < M_h < 190 \text{ GeV}$ [4].

3.5. $t\bar{t}h$ ($h \rightarrow b\bar{b}$)

This channel is attractive primarily due to the large branching ratio of $H \rightarrow b\bar{b}$ at $M_h < 130 \text{ GeV}$ (see Fig. 1). It is also relatively simple to trigger if one considers the semi-leptonic final state $t\bar{t}h \rightarrow \nu jj b\bar{b}b\bar{b}$, which provides a high- P_T isolated lepton and missing transverse energy, together with four b -jets. The channel has a complex final state, and thus there is a large combinatoric background which reduces the mass-peak resolution (Fig. 5). Additionally, there are several physics backgrounds to consider. The $t\bar{t}jj$ background requires ATLAS to optimise the light jet rejection fraction when b -tagging jets, whilst $t\bar{t}b\bar{b}$ appears generally through QCD gluon radiation (giving four b -jets in the final state). Kinematic information can typically be used to differentiate this background from signal, because the extra b -jets are not from a Higgs boson.

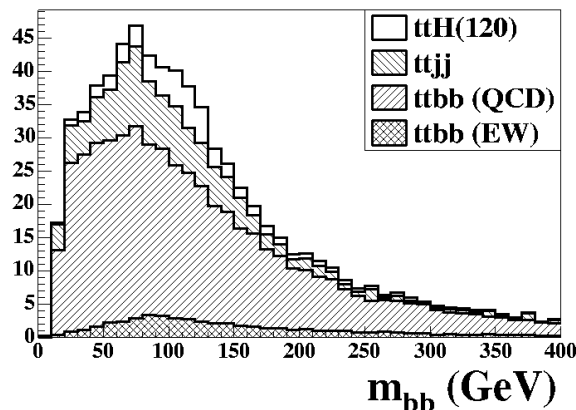


Fig. 5. Mass distribution for the $t\bar{t}h$ ($h \rightarrow b\bar{b}$) semi-leptonic final state with relevant backgrounds for an assumed $M_h = 120 \text{ GeV}$ and $\int Ldt = 30 \text{ fb}^{-1}$ [8].

The analysis selects events with a high jet multiplicity (≥ 6), and at least four b -tagged jets. The missing transverse energy is used to reconstruct the final state neutrino. The two W -bosons and top-quarks are required to be reconstructed (to remove background), and finally the remaining b -jets are combined to reconstruct the Higgs boson. The ATLAS analysis [8] has a significance of 2.4 for $M_h = 120 \text{ GeV}$, which falls as M_h increases (due to the rapid decrease in $H \rightarrow b\bar{b}$ branching ratio).

3.6. The MSSM Higgs discovery potential of ATLAS

In the MSSM at Born level, the Higgs sector phenomenology is determined by two parameters, the vacuum expectation value ratio of the two Higgs doublets $\tan\beta$, and the Higgs mass M_A . The M_h -max scenario (where SUSY parameters give the largest value for M_h) corresponds to the most conservative exclusion from LEP. The ATLAS discovery potential for this scenario is shown in Fig. 6. If $\tan\beta$ and M_A do in fact lie in the moderate $\tan\beta$ and large M_A region of Fig. 6, then only one Higgs boson will be found. In this case, other observables such as the ratio $BR(h \rightarrow WW)/BR(h \rightarrow \tau\tau)$ will be used to infer the possible existence of a supersymmetric Higgs sector.

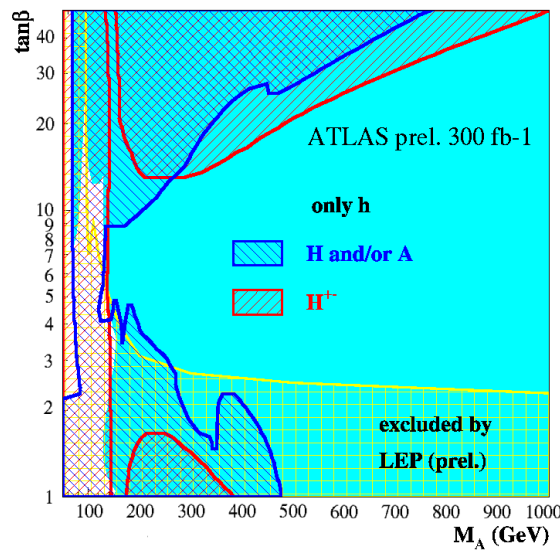


Fig. 6. ATLAS discovery potential for light and heavy neutral and charged Higgs bosons for $\int Ldt = 300 \text{ fb}^{-1}$ in the M_h -max scenario [9].

4. Conclusions

The ATLAS experiment has discovery potential for a SM Higgs boson over the mass range defined by the LEP exclusion limit of $M_h > 114.4 \text{ GeV}$ (95% C.L.) [10], to $\sim 1 \text{ TeV}$ [11]. A significant region of MSSM parameter space would yield discovery of multiple supersymmetric Higgs particles, should they exist.

References

- [1] The ATLAS Collaboration, CERN/LHCC/1999-14 and 15 (1999).
- [2] U. Aglietti et al., TeV4LHC Working Group, *Tevatron-for-LHC Report: Higgs*, hep-ph/0612172, 2006.

- [3] V. Barger et al., Phys. Rept. **286** (1997) 1.
- [4] S. Asai et al., Eur. Phys. J. C **32** S2 (2004) 19.
- [5] M. Bettinelli et al., ATL-PHYS-PUB-2007-013 (2007).
- [6] K. Cranmer et al., ATL-PHYS-2003-025 (2003).
- [7] C. P. Buszello et al., Eur. Phys. J. C **32** (2004) 209.
- [8] J. Cammin and M. Schumacher, ATL-PHYS-2003-024 (2003).
- [9] J. Haller, PoS HEP2005 (2006) 338.
- [10] The LEP Working Group for Higgs Boson Searches, Phys. Lett. B **565** (2003) 61.
- [11] N. Cabbibo et al., Nucl. Phys. B **158** (1979) 295.

MOĆNOST ATLASA ZA OTKRIĆE HIGSSA

Opisujemo tvorbu i raspade Higgasa u LHC-u i različite procese traženja ATLAS-om te dajemo pregled moćnosti ATLAS-a za otkriće Higgasa.